Small-scale modular windmill

Virginia Tech researchers have created and tested a mini wind turbine that is capable of charging small electronic devices and powering remote sensor networks.

**Scott Bressers,
Dragan Avirovik,
Chris Vernieri,
Jess Regan,
Stephen Chappell,
Mark Hotze,
Stephen Luhman,
Mickaël Lallart,
Daniel Inman and
Shashank Priya***

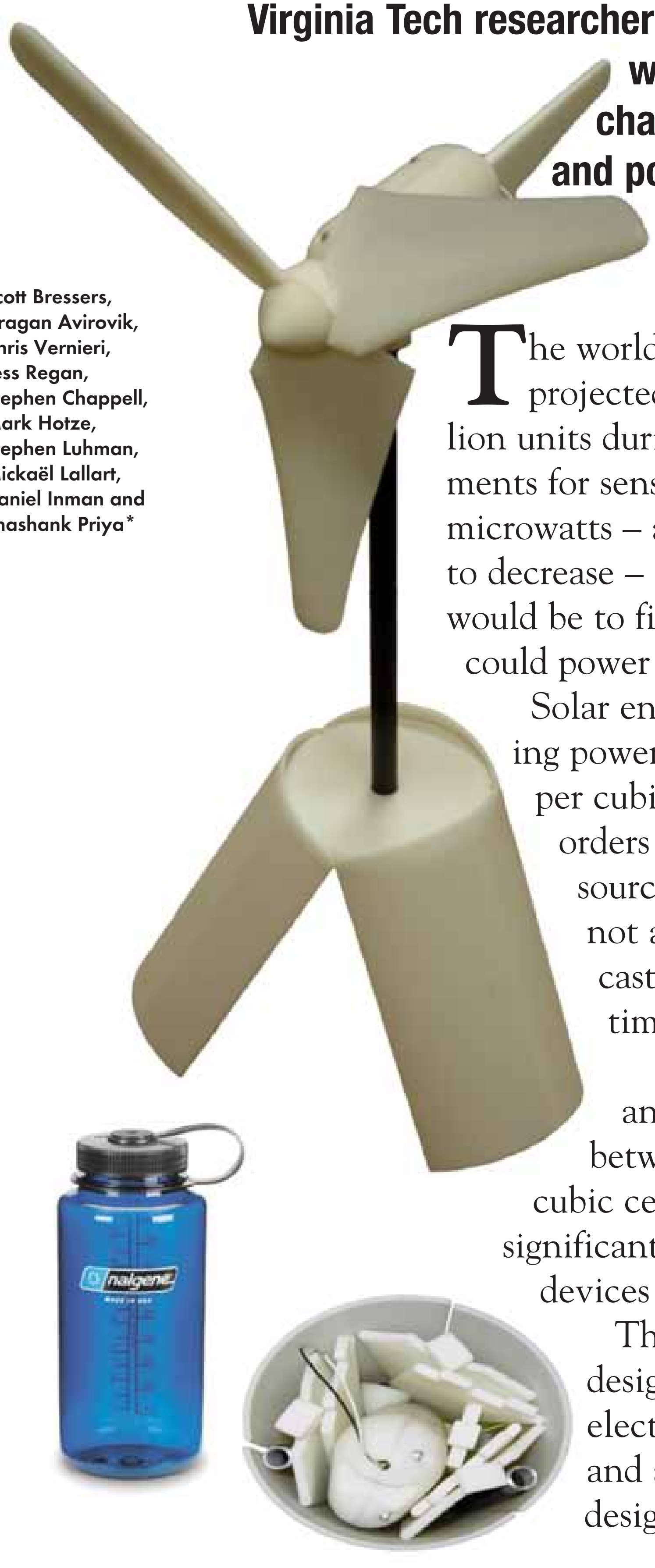

The worldwide ultra-low-power market is projected to reach more than 200 million units during 2010. Because power requirements for sensor nodes have decreased to 100 microwatts – and are expected to continue to decrease – an elegant solution to powering would be to find ambient energy sources that could power or replenish batteries.

Solar energy has the capability of providing power density of 15,000 microwatts per cubic centimeter, which is about two orders of magnitudes higher than other sources. However, direct sunlight is not always available because of overcast skies, shaded conditions or night time.

Air flow is an attractive source and possesses power density ranging between 300 and 350 microwatts per cubic centimeter. Thus, there has been significant interest in developing small-scale devices that can harvest air flow.

The conventional approach toward design of small-scale windmills uses electromagnetic-motor-based turbines and air-foil-based blade structures. We designed an optimized version of a

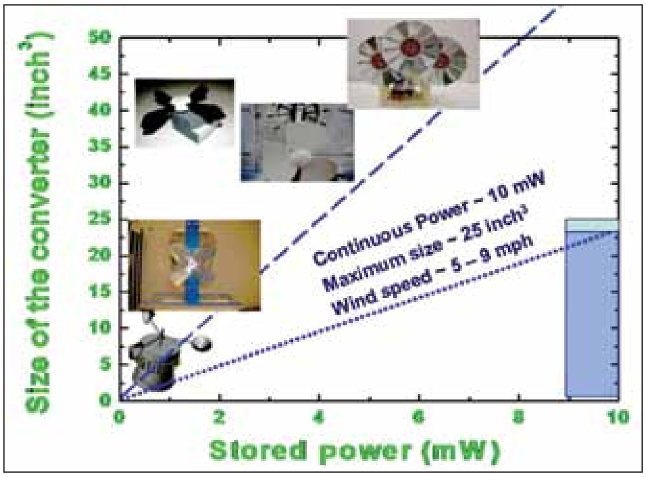

Fig. 1 Piezoelectric windmill research conducted at UTA.

small-scale windmill based on this conventional approach. We used a modular architecture and developed interfaces for integration with common mobile electronics, such as cell phones and iPods. The windmill generates 157 milliwatts at the nominal wind speed of 8 miles per hour and has a start-up speed of about 5 miles per hour. This power is attractive and suffices the needs for various mobile devices and structural health-monitoring networks.

Many wireless networks and sensor nodes require much less power. If that small power can be generated at start-up speeds of 1.5 to 2 miles per hour, than wind could become a viable alternative for an on-demand ubiquitous power source. This need has prompted research on an alternative to electromagnetic motors and generators. Windmills that use piezoelectric ceramics (bimorph transducers made from Pb(Zr,Ti)O_3), piezoelectric polymers (poly(vinylidene fluoride)), magnetoelectric composites (Pb(Zr,Ti)O_3/Metglas laminates) and coil/magnet assembly are being investigated.

Schmidt[1] described the idea of a piezoelectric wind generator using piezoelectric polymers in 1984. Calculations and experiments showed that an output power of a few milliwatts was possible for a reasonably sized windmill.[2] A "Piezoelectric Windmill" developed at the University of Texas at Arlington (Figure 1) showed the possibility of effectively capturing wind energy and generating electric power at a small scale.[3–5] One design used a 60-millimeter × 20-millimeter × 0.6-millimeter piezoelectric bimorph with a free length of 53 millimeters.[6]

A piezoelectric bimorph transducer structure was selected, because the force required for full deflection was small, charge developed under fully loaded condition was high, resonance frequency was very low and manufacturing cost was very low. The windmill charged a 0.1-farad capacitor with saturation at 5.5 volts for a continuous operating time of 30 minutes at 10 miles per hour wind speed. Robbins et al.[7] have performed calculations on piezoelectric-fiber-based composites in wind energy harvesting. They concluded that higher efficiencies could be obtained using flexible materials with higher coupling factors, such as piezoelectric fiber composites.

Others have used the flutter phenomenon and poly(vinylidene flouride) copolymer transducers to convert wind to electricity.

Still others designed and fabricated cost-effective small-scale windmills operating at low-wind-speed conditions for applications including weather-monitoring stations, remote highway-monitoring devices and security systems.

The demand from personal-electronics users for portable and effective battery charging is growing rapidly, because portable devices have limited operating time without regular charging. Users – hikers, campers, climbers, fishermen, bikers, skiers, backpackers and hunters – normally are not in the vicinity of the grid power supply and are fully dependent upon battery supply. However, the number of batteries that can be carried is limited and impose constraint on the operating time of devices. We propose a wind-power solution for these scenarios and demonstrate a modular wind turbine architecture that can generate up to 400 milliwatts at 10 miles per hour wind speed.

Because our wind-power solution is a low-altitude- or ground-based device, we had to overcome many challenges in its implementation. There is a natural boundary layer of flow over the surface of the earth because of viscous effects. This boundary layer causes lower wind speeds closer to the ground than those experienced at higher altitudes. The boundary layer near the earth is affected by the roughness of the surface. Therefore, a terrain with low-lying grass has a boundary layer with higher wind speeds closer to the ground than does a terrain of forest or building structures.

We used a power regression curve to estimate velocities in the boundary layer. We considered the kinetic energy of this moving air as it flows through the effective turbine area and, thus, estimated power of the wind.

Wind turbine design

A prime challenge in decreasing the size of a windmill is inefficiency in turbine structure that affects overall system performance. Turbine design for a 3-megawatt windmill is not necessarily the most efficient design for a small-scale windmill. A turbine produces power by slowing down the wind. The wind contains kinetic energy and, thus, imparts a force on the turbine blade. However, it is not a drag force that causes the turbine to spin. It is a lift force. As the blades move through the air, they experience two separate airstreams. The first air stream is from the wind itself hitting the plant form of the blade. The second air stream is caused by the blade moving through the air, similar to an airfoil on an airplane. The combination of these two airstreams produces the lift forces that keep the turbine in motion.

Betz's law is applied to determine how much the air speed must be slowed from the upstream velocity. The law states that a turbine's coefficient of performance is maximum when the downstream air velocity is one-third of the upstream velocity. The assumptions of this law are such that no rotor hub or an infinite number of blades with zero drag are impractical.

For a given blade size, the tip-speed ratio is defined as the ratio of the tip speed of the blades to the wind speed. This ratio is important because, for maximum efficiency, the wind turbine must spin at a rate that allows the electric motor to produce the most power. A higher tip-speed ratio is more efficient but requires blades to be designed such that they handle increased stresses.

Even with a high tip-speed ratio, gearing is necessary to step up the slower wind turbine and achieve the rotation required by the electromagnetic motor or generator. However, because any additional gear adds to the friction, it is best to minimize the gear ratio used in the design.

The number of blades in the windmill can be changed based on specific requirements of the design. After the number of blades is determined, the width of the blades must be calculated. Because the outer regions of the blade experience the most wind, the width of this section is more important than the inner regions. To increase the starting torque and turbine strength, the width of inner segments must not be overlooked. The blade setting angle – the difference between the striking angle of the apparent wind and the angle of attack of the blades – also must be considered.

The striking angle of the apparent wind is more toward the tip of the blade. Therefore, most blade designs are twisted to accommodate the flow characteristics of various parts of the blade. Even with a good blade design, there are losses that can influence the performance of any turbine. One of the principal losses that cannot be avoided is the wind that escapes around the outside of the blades. Even if the downstream air is slowed to one-third of the upstream velocity, the highest attainable coefficient of power is 0.593.

A problem known as tip loss also occurs, especially with designs that have fewer blades. Tip loss occurs when wind is directed around the blade tips where the bulk of the energy is captured. Turbines that have a low tip-speed ratio are affected by turbulent swirling coming off the blade. These power losses are the primary mechanical power losses that a typical turbine experiences. These losses must be added to the friction and electrical losses to determine the actual efficiency of the wind turbine.

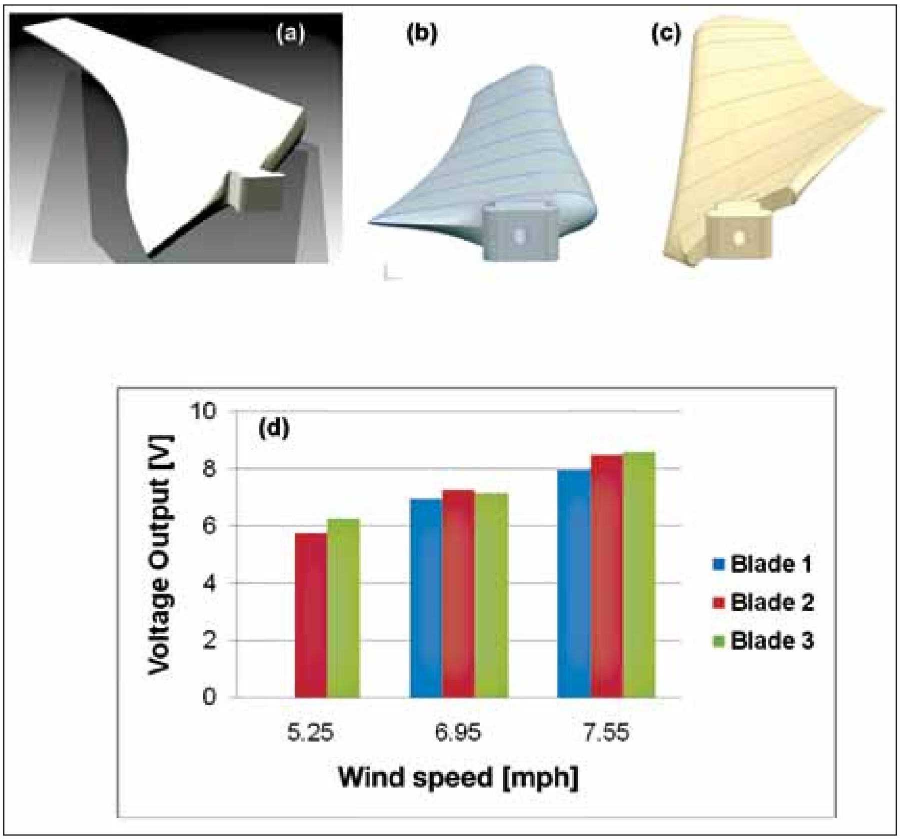

Fig. 2 Refined turbine blade designs. Dovetail pattern toward the base of the blade mates exactly to the hub. Blades in (a), (b) and (c) correspond to blades 1, 2 and 3, respectively, in (d), which is a comparative analysis of the blades.

The prototype we fabricated consisted of three subsystems. The rotor assembly includes the hub, hub cap and blades. The nacelle assembly houses the drive train and generator. The turbine base is considered as a subsystem, because it serves the role of packaging container.

Rotor assembly

The rotor assembly is encountered by wind-driven forces. It includes the turbine blades, hub to which the blades are attached and hub cap that holds the blades firmly in place. We designed a dovetail cutout pattern to achieve modularity in the hub.

The dovetail pattern serves two main purposes:

- It permits the turbine blades to be attached securely or removed easily.
- It allows the capability to replace the blades, provided they have specified dovetail pattern.

We selected a hub 1.5 inches in diameter, which allowed us to incorporate a 0.5-inch × 0.5-inch turbine blade cross section at the hub interface. We chose these important dimensions based on the overall scale of the wind turbine, that is, we attempted to keep it small but maintain stability. We used acrylonitrile butadiene styrene plastic material for fabrication and selected dimensions that had the strength needed to overcome wind forces exposed during operation.

The most crucial component of the rotor assembly and perhaps the entire wind turbine is the blade rotor. It is responsible for capturing the wind energy and transferring it to the drive train via rotational inertia. Our initial designs used a combination of cues taken from large- and medium-scale wind turbine blades as well as airfoil

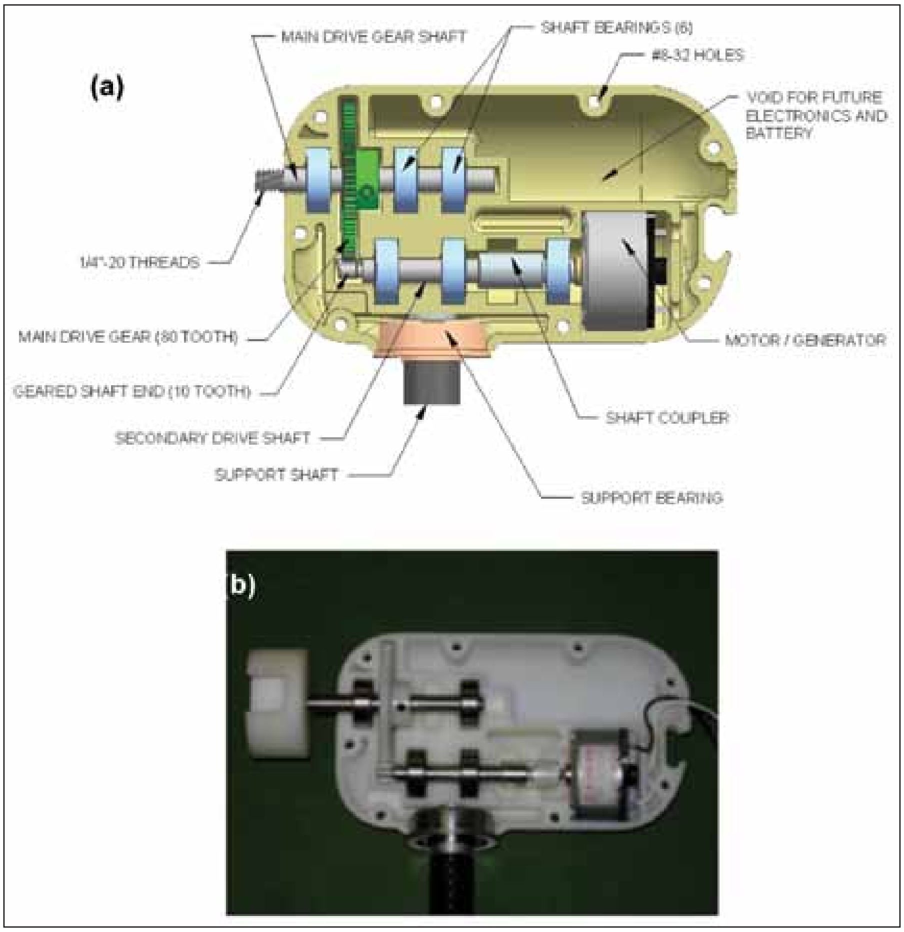

Fig. 3 Nacelle subassembly (a) diagram that shows all internal parts and (b) photograph of the fabricated prototype with its integrated dc electric motor.

shapes in general. We found the ultimate selection of geometry through a synthesis of aerodynamic laws that predict lift and drag characteristics.

We used an automated computational code from a commercial vendor (windstuffnow.com) that incorporates mathematical models for blade design. Figure 2 shows the refined version of turbine blade designs that we considered and that were derived from the computational code.

The length of the blade is 6.75 inches, which, including the mounting end section, is 7.5 inches. As with most wind turbine blade designs, the airfoil chord length is gradually shortened along the length of the blade. Lesser blade area is required near the blade tip because of the rotational nature of the blade. Moreover, the tip travels faster than the base and, thus, requires less blade area to capture an equivalent amount of wind energy.

Figure 2(d) shows the comparative analysis of the blades. Blade (c) exhibits higher performance in the wind range under consideration. Figure 2(d) also shows the start-up speed for each of the blade designs. Other design features of the blade include the base pattern, hollow blade core and twisting overall blade geometry.

An initial small angle is necessary at the base portion of the blade such that, as wind impacts the blade, the blade naturally tends to rotate in a direction perpendicular to the wind flow. The angle of twist increases and moves along the length of the blade toward the tip. The wind's relative angle of attack changes because of the rotational motion of the blade through the air. More angle of twist is needed toward the blade tip to compensate for this increased angle of attack caused by increased blade speed.

The base pattern of the turbine blade must match in geometry with that of the hub for the interchangeable dovetail system to be effective. We added a cylindrical hollow blade core to the hub. This hollow core has a diameter of 0.17 inch and accepts an epoxy-coated 0.158-inch-diameter carbon fiber tube. Because the ABS plastic blade has a relatively small thickness, the addition of the carbon fiber tube provides added strength, durability and rigidity to the blade. It proves to be a novel design concept for a turbine blade of this scale. We used a dome-shaped hub cap to adhere the turbine blades to the hub.

The hub cap, blades and rotor form a modular system that can be assembled easily. Threaded screws and friction mounting are important aspects of the modular nature. Another modular feature is the blade-mounting scheme in which a T-slot recess is designed into the hub to allow quick and secure installation or removal.

Nacelle assembly

The nacelle assembly houses the electronics, gearing and motor. The nacelle also forms the support structure onto which the rotor and base assemblies are attached. The rotor assembly is attached through a shaft that connects the rotor hub to the gearing components inside the nacelle. This mechanical connection takes place through the 0.125-inch-diameter hole toward the front of the nacelle, as shown in Figure 3.

The flowing aerodynamic shape of the nacelle structure, which transitions from a circular profile to a slender oval-shaped profile, enables many structural and mechanical functions. We selected this profile to meet the dual objectives of minimizing air drag and providing enough internal volume to fit all of the wind turbine components. The profile suggests that more volume is available near the circular side of the nacelle, where the motor and gear components are installed. However, the volume toward the other side of the nacelle is reduced and elongated to form a tail fin shape, where the electronics are housed. We chose this transitional geometry, because the electronics are generally smaller and flatter in nature than the mechanical components.

A fin-shaped rear section allows the wind turbine to align with the wind. This self-aligning feature is critical to the efficient operation of the wind turbine. It forces the turbine blades to align directly into the strongest wind flows and, thus, capture the maximum amount of wind energy available.

It is ideal to have the wind turbine and the nacelle structure elevated above of the ground as much as possible. Therefore, a support shaft is needed. Two 6-inch-long carbon-fiber tube shafts that have a 0.58-inch outer diameter are connected together with a coupling to provide a 12-inch total distance between the nacelle and base assemblies. This carbon-fiber material is well suited for this application because of its light weight, rigidity and strength.

The interconnection between the nacelle and the support shaft is a flanged ball bearing. This 1.125-inch-outer-diameter bearing is inserted into a counterbored hole molded into the nacelle with dimension equal to the ball bearing's outer diameter. The location of the counterbore is based on the overall weight balance of the components mounted onto the support shaft. We chose the location to lie along the nacelle's plane of symmetry and near the front half of the nacelle, where the weight is heaviest. We chose the ball-bearing mounting scheme to allow a solid connection between support shaft and nacelle, and because this type of bearing provides minimal rotational friction.

The windmill components and an assembled windmill are shown in Figure 4.

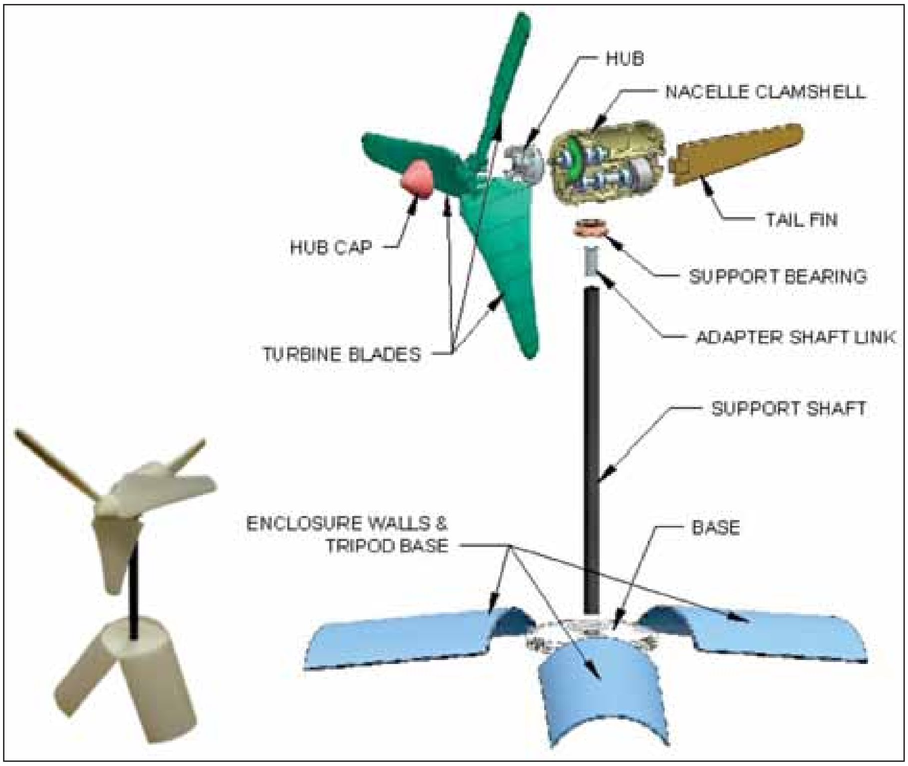

Fig. 4 Fully assembled windmill prototype and exploded windmill assembly showing detail of components.

Device packaging and modularity

The size and weight limitations of the windmill require innovative designs for all of the components. Each component was designed using materials and sizes such that the entire windmill can be contained within a 2-liter volume. The wind turbine can be assembled on demand by the end user. Accordingly, the design consists of few components. We selected a three-segment enclosure design that provides the material for the outer container packaging of the wind turbine and serves as its base. We used a hinged design so that the outer walls of the wind turbine container fold down through 90°of rotation to form a sturdy tripod base.

After the sidewalls are folded, the wind turbine base is formed by flipping the entire container assembly such that the sidewalls are oriented in a concave-down fashion. This folding action forms a tripod-style base that is inherently stable because the sidewalls are hinged on the base plate.

Power converter

The power-generating motor, gearing components, battery and power management circuitry are contained within the aerodynamically designed nacelle. The nacelle design was constrained by the target size of the container, but had to be large enough to incorporate the 8:1 gear ratio from the propeller to the generator.

Two shafts are secured within the nacelle housing and are free to rotate on ball bearings that rest in grooves built into the housing mold. The large gear on the propeller shaft mates with the smaller gear on the generator shaft. The generator spins eight revolutions while the blade spins one. The generator fits snugly within a larger groove in the mold. Two leads come out of the generator at the rear of the nacelle to test its power output. The nacelle is free to swivel on carbon-fiber hollow rods by a ball bearing mounted at its bottom. The ends of the rod are threaded to fit securely to the bottom of the nacelle and to attach to the wind turbine base.

Prototype assembly

The wind turbine blades are perhaps the most material-sensitive components. Therefore, the selection of materials is a fine balance between strength and weight. Although this type of performance tradeoff is evident for other components of the wind turbine device, it is absolutely crucial that the turbine blades are robustly designed. Typically, high-strength and durable materials are required when a sturdy and robust design is needed. This is true for turbine blades. However, material weight is a more important issue than strength

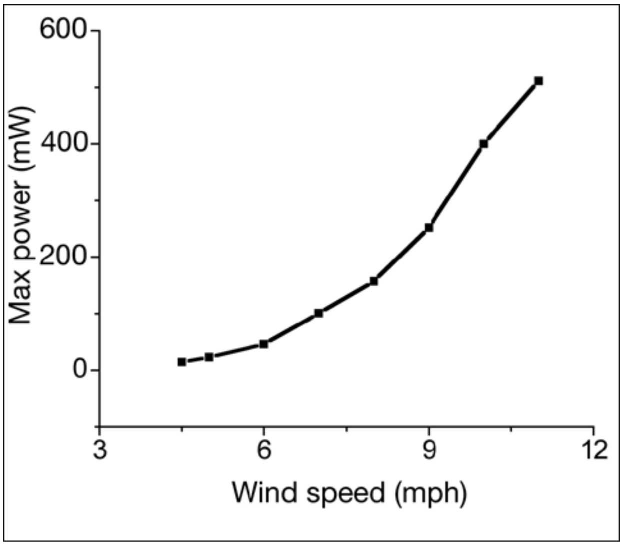

Fig. 5 Maximum power produced by small-scale windmill at relatively low wind speeds.

in the applications considered here.

Therefore, lightweight materials must be used with innovative blade geometries that provide a measure of blade reinforcement. Lightweight poly(vinyl chloride) plastic was selected as the blade material, because it can be easily manufactured using rapid-prototyping, has a comparatively high strength to weight ratio, is generally lightweight, and can be formed easily and inexpensively. Plastic is not as strong as metals or other exotic materials. However, a creative blade geometry that places more material in the most stress prone areas may provide a way to compensate for certain strength deficiencies.

Optimal load resistance

We tested our prototype at various wind speeds using a low-speed, laminar wind tunnel. The wind turbine includes a direct-current generator (Mabuchi RF-500TB-14415) that features permanent magnets operating in generator mode. A range of shunt resistors was used as an electrical load to the dc generator to determine the optimal resistance for the windmill. We took a resistor sweep of each wind speed in the range of 100 ohms to 3 megaohms, and the power produced by the turbine was calculated.

We conducted measurements (Figure 5) over a wind speed range of 4.5 to 11 miles per hour. We measured the variation of output power as a function of the resistance for various wind speeds. Optimum resistance – the electrical load at which maximum output power was measured for a given wind speed – decreased with increased wind speed. It ranged from 1,300 to 100 ohms for wind speeds in the range of 4.5 to 11 miles per hour. Decreased optimal resistance was a result of decreased generator internal inductance and equivalent electrical resistance, which varied as a function of generator rotational speed.

Rotational speed

We measured the rotational speed of the blades and correlated this data to the magnitude of external load resistance. We discovered that the rotational speed exhibited a rather steep slope over the resistance range 100 to 600 ohms. However, the rotational speed saturated for resistances greater than 600 ohms. The relationship between rotational speed and wind speed at optimal resistance demonstrated a proportional increase in rotational speed as wind speed increased.

Power versus wind speed

We used the optimum load resistance to create a power versus speed curve. The windmill generated 100 milliwatts at a nominal wind speed of about 7 miles per hour. The power increased to 500 milliwatts at a wind speed of 11 miles per hour.

Electrical interface

We then investigated the most efficient interface for maximizing the power output of the small-scale wind turbine. First, we prepared an analysis of the electrical model of the wind turbine. Second, we determined the power optimization based on a dc/dc converter operating in discontinuous mode. Third, we used, as an example, the application of the wind turbine to cell-phone charging.

Power maximization

For a given generator, the power is maximized at a particular load value. However, the wind turbine is rarely connected to this optimal load. Therefore, an additional electrical interface is required for proper opera-

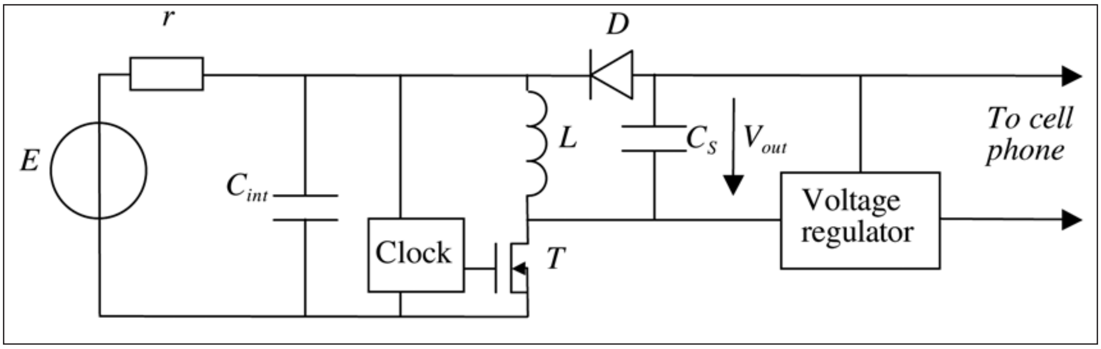

Fig. 6 Diagram of windmill electrical circuit used for charging a cell phone: E is the electrical generator; r is the loss resistor; C_{int} is the internal capacitor to smooth generator output; T is the switching transistor; L is the inductance; D is the diode; and C_s is the smoothing capacitor. V_{out} is the output voltage.

tion of the device. We use a buck-boost dc/dc converter operating in discontinuous operation, which allows us to maintain a constant load across the output. The principles of operations consist of switching the generator output to an inductor with a high frequency and a duty cycle. The switching is done using a negative metal oxide semiconductor transistor coupled with a low-power clock. An additional capacitor is used for smoothing the generator output.

When the generator is connected to the inductance, energy is transferred to the inductance. When the transistor is blocked, the electromagnetic energy stored by the inductance is released to the load and smoothing capacitor. A diode is used to ensure a proper energy flow from the inductance to the load and output-smoothing capacitor.

During the energy transfer from the generator to the inductance the current flows through the inductance. Hence, the mean current flowing from the generator is in steady state with the current supplied by the capacitor over a time period and is the same as the current absorbed by the capacitor.

Therefore, we can properly tune the converter parameters (inductance, switching frequency and duty cycle) so they equal the optimum resistance for energy extraction enhancement. This allows harvesting the maximum power from the generator. This extracted power then is transferred to the load and smoothing output capacitor in the second conduction stage. However, such an analysis only applies when the converter operates in discontinuous mode.

Application

We use the currently proposed electrical interface. However, an additional voltage regulator is required to comply with the 5-volt input voltage of the cell-phone battery, as shown in the schematic depicted in Figure 6. The clock (OV-1564-C2, Micro Crystal, Switzerland) features a switching frequency of 32 kilohertz with a duty cycle of 50 percent. It consumes less than 0.5 microamperes for an input voltage from 1.2 to 5.5 volts.

The voltage regulator (Motorola MC78LC50HT1) features a regulated output voltage of 5 volts and requires a typical quiescent current of 1.1 microamperes. The switching transistor is a NMOS (Motorola 2N7000) with a threshold voltage of 3 volts and a "on" resistance of 5 ohms, which allows decreasing the losses during the energy transfer from the generator to the inductance. The diode (BAT46, STMicroelectronics) has a very low forward voltage of 0.25 millivolts. The size of the interface is easily embeddable, even using off-the-self components.

Protoype

Our prototype (see Figure 7) operates in discontinuous mode and features low-power components. It was used to successfully charge a cell-phone battery from a constant, low-speed wind source. This serves as a proof-of-concept for the potential of applying large-scale wind turbine design to small-scale models for the purpose of powering small electronics in remote locations. Moreover, this prototype is portable and cost effective; making consumer products feasible. ■

Acknowledgment

The authors gratefully acknowledge the financial support from NIST and CEHMS.

About the authors

Scott Bressers, Dragan Avirovik, Chris Vernieri, Jess Regan, Stephen Chappell, Mark Hotze, Stephen Luhman, Mickaël Lallart, Daniel Inman and Shashank Priya are research staff members with the Center for Energy Harvesting Materials and Systems and the Center for Intelligent Material Systems and Structures, Department of Mechanical Engineering, Virginia Tech, Blacksburg, Va.

Fig. 7 Photograph a cell phone connected to the electrical charging circuit of the windmill.

References

[1] V.H. Schmidt, "Piezoelectric Wind Generator," U.S. Pat. No. 4 536 674, 1984.

[2] V.H. Schmidt, "Piezoelectric Energy Conversion in Windmills"; pp. 897–904 in *Proceedings of 1992 IEEE Ultrasonics Symposium*.

[3] S. Priya, C. Chen, D. Fye and J. Zhand, "Piezoelectric Windmill: A Novel Solution to Remote Sensing," *Jpn. J. Appl. Phys.*, **44**, 104 (2004).

[4] S. Priya, "Modeling of Electric Energy Harvesting Using Piezoelectric Windmill," *Appl. Phys. Lett.*, **87**, 184101 (2005).

[5] C. Chen, R. Islam and S. Priya, "Electric Energy Generator," *IEEE Trans. Ultrason. Ferroelec. Freq. Contrl.*, **53** [3] 656–61 (2006).

[6] R. Myers, H. Kim, H. Stephanou and S. Priya, "Small Scale Windmill," *Appl. Phys. Lett.*, **90**, 054106 (2007).

[7] http://www.mech.unimelb.edu.au/people/staff/marusicpublications/IMECE2006%20Draft2.pdf